Misalignment Considerations in Laser Diode to Circular Core Graded Index Single Mode Fiber Excitation via Upside Down Tapered Microlens on the Fiber Tip

Sumanta Mukhopadhyay [a, b]

[a] Department of Physics, St. Paul's Cathedral Mission College, 33/1 Raja Rammohan Roy Sarani, Kolkata-700009,West Bengal, India

[b] Fiber Optics Research Group, Department of Electronic Science, University of Calcutta, 92 A.P.C. Road, Kolkata -700009, West Bengal, India

Email: sumukherjee_74@yahoo.com

Date of Submission: 5th June, 2015 Date of Acceptance: 10th June, 2015

Abstract

By employing Gaussian field distributions for both the source and the fiber and also the derived ABCD matrix for upside down tapered microlens under paraxial approximation, we investigate theoretically the coupling optics involving laser diode emitting practically interesting wavelengths of 1.3 μm and 1.5 μm, respectively and a series of circular core graded index single mode fibers with different refractive index profile exponents via upside down tapered microlens on the fiber tip in presence of possible transverse and angular misalignments. Further, it is observed that out of the studied refractive index profiles, triangular index profile having the dispersion-shifted merit comes out to be the most suitable profile to couple laser diode to such abovementioned fiber for two wavelengths of practical interest. Our formalism is very simple in comparison to the other existing methods involving cumbersome numerical integrations. The results are extremely useful for assessing deeply the sensitivity of such coupler with reference to above kind of misalignments. Such analysis which as per our knowledge is the first theoretical investigation, will be extremely important for the design of optimum launch optics involving circular core graded index single-mode fiber.

Keywords: Circular core graded index fiber, Upside down tapered microlens, Optical coupling, Transverse misalignment, Angular misalignment

1. Introduction

Optical packaging of semiconductor laser diode (LD) requires high coupling efficiencies and large misalignment tolerances for making the devices easier to handle, more reliable and more rugged from the point of view of its application based orientation such as pumping erbium-doped optical fiber amplifiers and optical communication systems. For a highly efficient laser, usage of microlensed fibers are very common in practical semiconductor laser packages [1]. However, the advantage of alignment free and miniature optical design between the microlens and the fiber, demands the development of microlens on the fiber tip. The advantage of the design of more-compact optical components and modules also makes the design and fabrication of fiber microlens vitally attractive. Therefore, the fabrication and design of microlenses on the fiber tip are of tremendous importance as far as source to single mode fiber (SMF) coupling is concerned [2-15]. These microlenses which are either hemispherical or conical in shape have the common advantage of being self-centered.

In this respect, a hyperbolic microlens [2,3,4] on the tip of a SMF has been shown to be most effective coupler in comparison to other types of conventional coupling systems using hemispherical [2,3], parabolic [5,6] microlenses. Estimations of coupling optics in case of LD to circular core step index single mode fiber (CCSISMF) excitations via hyperbolic microlens [7-9], hemispherical microlens [10,11], parabolic microlens [5,6] on the fiber tip in absence and presence of transverse and angular misalignments have been previously reported based on concerned ABCD matrix formalism. It may be relevant to mention in this connection that analysis of the coupling optics involving a LD to a hyperbolic microlens [12,13] hemispherical microlens [14,15] on the tip of an elliptic core step index single mode fiber (ECSISMF) in absence and presence of possible misalignments have been reported recently.

But the coupling efficiency of hemispherical microlens as well as parabolic microlens is impaired due to limited aperture while fabrication of hyperbolic microlens is limited by involved technique.

Recently upside down tapered microlens (UDTM) on the fiber tip, designed by tapering the fiber end, has also emerged [16-18] side by side as a new lensing scheme in coupling optics. Therefore, the study of coupling optics involving UDTM on the tip of SMF is of huge importance. This novel lensing scheme, UDTM [17-19] can be drawn from the fiber end where the fiber tip is tapered into a large hemispherical shape. UDTM may be utilized to accumulate a huge amount of light from the source [17]. A detailed work on formation and power distribution properties of UDTM has been already reported [17] while the corresponding structure of the UDTM fiber end and the refractive index distribution has already been highlighted [18]. The transformation ABCD matrix of the UDTM developed on CCSISMF end has already been prescribed [19]. It is to be noted that in case of semiconductor LD emitting light of wavelength $1.3\mu m$, the coupling efficiency between the LD with a CCSISMF via a uncoated UDTM on the tip of the step index SMF comes out to be 97% [20]. Moreover, the study of the coupling losses in absence and presence of possible transverse and angular mismatches in case of LD to ECSISMF coupling via UDTM on the fiber tip has already been reported [21]. It deserves mentioning in this connection that the Fresnel backward reflection can be neglected to investigate the coupling efficiencies in case of coated UDTM on the tip of the CCSISMF [19,20] and ECSISMF [21] .

Again, we know that graded index fibers (GIF) are tremendously important due to its low sensitivity to micro- and macrobending. Side by side, a GIF have high bandwidth. Despite numerous studies on different types of microlens on the tip of step index SMF, very recently study on hyperbolic microlens [22] and hemispherical microlens [23] on the tip of circular core graded index single mode fiber (CCGISMF) have already been reported. However, no such information is available regarding a study of coupling optics involving LD and CCGISMF via UDTM on the fiber tip. However, it is pertinent that one should know the exact nature of a refractive index profile to support maximum coupling between LD and UDTM not only developed monolithically on the CCGISMF but also on the GIF to be attached with a SMF. Such investigation, reported for the first time to the best of our knowledge, is important from the standpoint for assessing the sensitivity of the said coupler in presence of the said two kinds of mismatches. Such a study, therefore, should deserve the immediate attention of experimentalists.

Actually, as in conventional splicing of two fibers, one cannot avoid the possible misalignment [24]. Although it is expected that the UDTM on the fiber tip should be formed at the ideally set position as illustrated in Figure 1, it may be difficult to achieve the same precisely in practice. Further, the limitations of fabrication of the said type of coupler may lead to relative shift between the microlens output and the fiber input faces resulting in two possible misalignments, namely, transverse and angular mismatches. Thus, the losses are also incurred due to two type of misalignments while we couple light via UDTM through a SMF. Our aim is to study the coupling losses due to possible transverse and angular mismatches in the case of a LD-to-CCGISMF coupling via a UDTM on the fiber tip. Such investigation is important and pertinent for assessing the sensitivity of the efficient coupler in the presence of the two kinds of misalignments.

This paper initially deals with the theoretical investigation of the coupling efficiencies between a semiconductor LD emitting light of wavelength $\lambda = 1.3\ \mu m$ [4] and $\lambda = 1.5\ \mu m$ [4] and a series of CCGISMFs with different profile exponents in refractive index profile [22,25] via UDTM on the tip of these fibers in absence of possible transverse and angular mismatches. The results between these two cases are compared. Finally, the angular and transverse misalignments are studied for the most suitable fiber having a specific profile exponent in refractive index profile excited with two LDs emitting light of a particular wavelength. As stated earlier, this analysis is based in the framework of previously formulated [19,20] simple ABCD matrix method for refraction by a upside down tapered interface. In fact, prediction of coupling optics by ABCD matrix formalism has produced excellent results as far as coupling of LD via UDTM on the tip of CCSISMF [19,20] as well as on the tip of ECSISMF [21] is concerned. Concerned calculations are easily executable with very little computations.

Thus, in this paper, we theoretically predict the coupling losses in separate cases of possible transverse and angular mismatches using simple ABCD matrix formalism for refraction by a upside down tapered interface [19,20] in the case of LD-to-CCGISMF excitation via a UDTM on the fiber tip. In this connection, the Gaussian approximation of field distributions for both the source and the fiber are employed and calculations are restricted to paraxial approximation. The relevant calculations are executable with little computations. The results will be extremely important in the study of optimum launch optics involving specifically CCGISMF.

2. Analysis

2.1. Preview of UDTM structure and spot sizes of CCGISMF

In this analysis, we consider the structure of the UDTM fiber end drawn from a SMF of core radius '*a*' as shown in Figure1. Here, the radius of curvature R_0 and height '*h*' of the spherical end are related to the radius of aperture '*d*' by [18, 19]

$$R_0 = \frac{h^2 + d^2}{2h} \quad \ldots.. \quad (1)$$

where the radially symmetric axis OZ is actually the fiber axis and *z* and *r* represent the respective axial and radial coordinates, in the tapered region. The tapered surface equation is given by [18,19]

$$r = d\left(1 - \frac{z}{L}\right) \quad \ldots\ldots (2)$$

where *L* is the length of the cone including the tapered region.

For graded index profiles, the refractive index distribution is written as [25]

$$n(r) = n_{core}\left[1 - 2\left(\frac{r}{a}\right)^g \Delta\right]^{0.5} \quad \text{for } r < a$$

$$= n_{clad} = n_{core}\left[1 - 2\Delta\right]^{0.5} \quad \text{for } r >= a \ldots\ldots\ldots\ldots..(3a)$$

where *g* is the exponent of power law, and Δ, the grading parameter is defined as

$$\Delta = \frac{n_{core}^2 - n_{clad}^2}{2n_{core}^2} \quad \ldots\ldots\ldots\ldots\ldots\ldots\ldots\ldots..(3b)$$

where n_{core} and n_{clad} being refractive indices of core axis and cladding, respectively.

It may be noted that *g* = 1, 2 and ∞ correspond to triangular, parabolic and step profile distributions respectively.

Again, the normalised frequency *V* is given by $V = k_0 a\left(n_{core}^2 - n_{clad}^2\right)^{\frac{1}{2}}$ with k_0 being the free space wave number.

Further, the Gaussian beam width parameter w_f for CCGISMF as a function of normalised frequency *V* and the exponent *g* of the power law profile is approximated as [25]

$$\frac{w_f}{a} = \left[\frac{A'}{V^{2/(g+2)}} + \frac{B'}{V^{3/2}} + \frac{C'}{V^6}\right] \ldots\ldots\ldots\ldots\ldots\ldots (4)$$

where parameter optimisation of the functions leads to expressions for A', B' and C' given as [25]

$$A' = \left\{ \frac{2}{5} \left[1 + 4\left(\frac{2}{g} \right)^{5/6} \right] \right\}^{1/2} \ldots\ldots\ldots\ldots\ldots\ (5a)$$

$$B' = e^{0.298/g} - 1 + 1.478(1 - e^{-0.077g}) \ldots\ldots\ldots\ldots(5b)$$

$$C' = 3.76 + \exp\left(4.19/g^{0.418}\right) \ldots\ldots\ldots\ldots\ldots\ldots(5c)$$

with their validity for $1.5<V<\infty$.

It must be noted that the fiber spot size w_f is approximated for step index fiber as [26]

$$w_f = a\left[0.65 + \frac{1.619}{V^{1.5}} + \frac{2.879}{V^6} \right] \ldots\ldots\ldots\ldots\ldots\ldots\ldots(6)$$

2.2. Formulation of microlens coupling scheme

The coupling scheme to be studied has been presented in Figure 1. Here , 'u' is the distance of separation between the UDTM end of the fiber and the LD. Elliptical intensity profiles of the optical beams emitted from LD are approximated by Gaussian spot sizes w_{1x} and w_{1y} along two mutually perpendicular directions, one perpendicular and the other parallel to the junction planes. Again, in our analysis we use some usual approximations [2,7-15,19-21] like no transmission loss, Gaussian distributions for both the source field and the fiber field, perfect matching of the polarisation mode of the fiber field and that on the microlens surface, sufficient angular width of the microlens for the interception of entire power radiated by the source for typical values of the microlens parameters employed. However, for the purpose of estimation of coupling optics using such source and various kind of microlenses [7-15,27], we simply use Gaussian beam with the elliptical waist spot sizes since the laser sources we usually employ have dimensions of the parallel and perpendicular junctions fairly comparable [20].

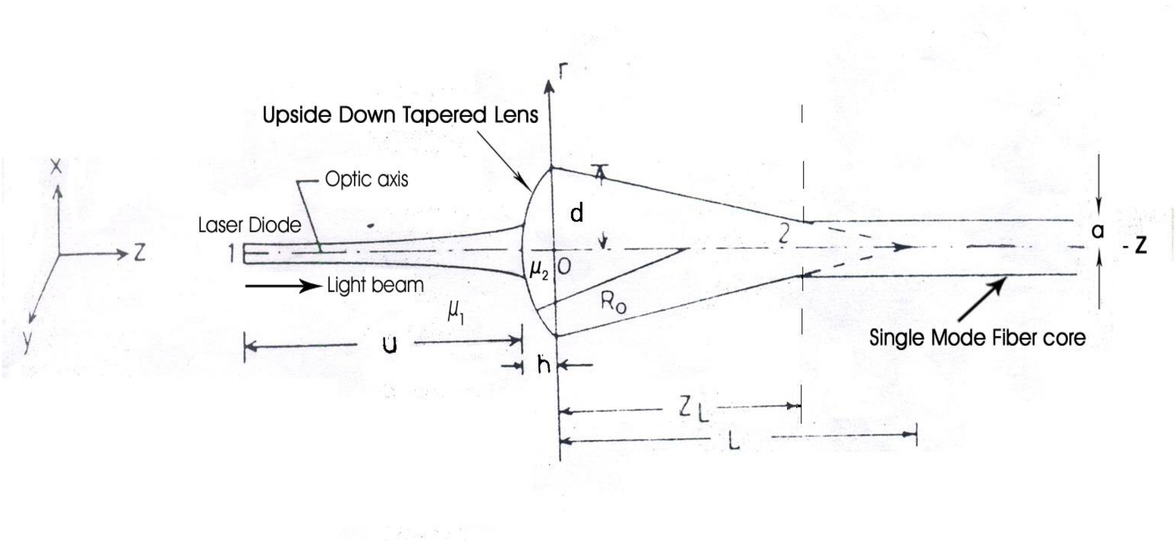

Figure 1: Geometry of laser diode to circular core single mode fiber coupling via upside down tapered microlens on the fiber tip ; μ_1 and μ_2 stand for refractive indices of incident and microlens media respectively.

The field Ψ_u representing the output of the LD at a distance u from the UDTM surface is taken as [7-15,28]

$$\Psi_u = \exp\left[-\left(\frac{x^2}{w_{1x}^2}+\frac{y^2}{w_{1y}^2}\right)\right]\exp\left[-\frac{ik_1}{2}.\frac{x^2+y^2}{R_1}\right] \ldots\ldots\ldots\ldots\ldots(7)$$

Here, w_{1x} and w_{1y} represent the spot sizes along two perpendicular directions X and Y, k_1 is the wave number in the incident medium and R_1 is the radius of curvature of the wavefronts from the laser source. Our analysis is applicable to single frequency laser emitting only one spatial mode with a Gaussian intensity profile.

It is already known that Gaussian approximations for fundamental mode in CCSISMF [7-11,20] represent sufficiently accurate results in the context of coupling losses. The corresponding fundamental modal field in such fiber is taken as [26]

$$\Psi_f = \exp\left[-\frac{x^2+y^2}{w_f^2}\right] \ldots\ldots\ldots\ldots\ldots\ldots\ldots\ldots(8)$$

where w_f being the fiber spot size corresponding to Eqs. (4) and (5a-5c) for CCGISMF and Eq. (6) for CCSISMF.

The UDTM transformed laser field Ψ_v on the fiber plane 2 as indicated in Figure 1 can be expressed as [28]

$$\Psi_v = \exp\left[-\left(\frac{x^2}{w_{2x}^2}+\frac{y^2}{w_{2y}^2}\right)\right]\exp\left[-\frac{ik_2}{2}\left(\frac{x^2}{R_{2x}}+\frac{y^2}{R_{2y}}\right)\right] \ldots\ldots\ldots\ldots\ldots\ldots(9)$$

where k_2 is the wave number in the microlens medium and w_{2x}, w_{2y} are respectively microlens transformed spot sizes and R_{2x}, R_{2y} being the respective transformed radii of curvature of the refracted wavefronts in the X and Y directions. The method of finding w_{2x}, w_{2y}, R_{2x} and R_{2y} in terms of w_{1x}, w_{1y} and R_1 with the relevant ABCD matrix for UDTM [19,20] on the fiber tip is once again presented in the Appendix for ready reference.

The source to fiber coupling efficiency via UDTM on the fiber tip is expressed in terms of well known overlap integral as mentioned below [7-11,27,28]

$$\eta = \frac{\left|\iint \Psi_v \Psi_f^* dxdy\right|^2}{\iint |\Psi_v|^2 dxdy \iint |\Psi_f|^2 dxdy} \ldots\ldots\ldots\ldots\ldots\ldots\ldots\ldots(10)$$

Therefore η_0 for circular core fiber is given by

$$\eta_0 = \frac{4w_{2x}w_{2y}w_f^2}{\left[\left(w_f^2+w_{2x}^2\right)^2+\frac{k_2^2w_{2x}^4w_f^4}{4R_{2x}^2}\right]^{1/2}\left[\left(w_{2y}^2+w_f^2\right)^2+\frac{k_2^2w_{2y}^4w_f^4}{4R_{2y}^2}\right]^{1/2}} \quad \textbf{.................(11)}$$

However, Eq.(11) can be obtained by employing Eqs. (8) and (9) in Eq. (10) [7-11,22].

2.3. Misalignment considerations:

Now, the evaluation of the coupling efficiency in the presence of transverse misalignment in the X-Y plane is based on the assumption that the center of the fiber is shifted to a point having coordinates (d_1,d_2) as shown in Figure 2.

In this case, the fundamental mode of the fiber can be represented as [9,11,28]

$$\psi_f = \exp\left[-\left(\frac{(x-d_1)^2}{w_f^2}+\frac{(y-d_2)^2}{w_f^2}\right)\right] \quad \text{..........................(12)}$$

Employing Eqs. (9), (10) and (12), one can obtain the coupling efficiency for only transverse misalignment as [9,11,22]

$$\eta_t = \eta_0 \exp\left[\frac{2d_1^2}{w_f^2}\left\{\frac{w_{2x}^2\left(w_{2x}^2+w_f^2\right)}{\left(w_f^2+w_{2x}^2\right)^2+\frac{k_2^2w_{2x}^4w_f^4}{4R_{2x}^2}}-1\right\}\right]\exp\left[\frac{2d_2^2}{w_f^2}\left\{\frac{w_{2y}^2\left(w_{2y}^2+w_f^2\right)}{\left(w_f^2+w_{2y}^2\right)^2+\frac{k_2^2w_{2y}^4w_f^4}{4R_{2y}^2}}-1\right\}\right] \text{.. (13)}$$

where η_0 for circular core fiber is given by Eq. (11).

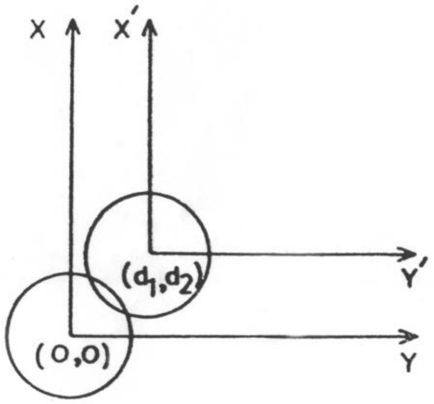

Figure 2: Transverse misalignment between the imaged laser spot and the center of the fiber.

We present the angular misalignment of a small angle θ between the UDTM transformed end face and the entrance of the fiber in Figure 3. The microlens transformed field on the fiber can be approximated as [9,11,22]

$$\Psi_v = \exp\left[-\left(\frac{x'^2}{w_{2x}^2}+\frac{y'^2}{w_{2y}^2}\right)\right]\exp\left[-\frac{ik_2}{2}\left(\frac{x'^2}{R_{2x}}+\frac{y'^2}{R_{2y}}\right)\right]\exp(ik_2 x'\theta) \quad \text{.............(14)}$$

Accordingly the fundamental mode of the fiber is expressed as [9,11,22]

$$\Psi_f = \exp\left[-\left(\frac{x'^2+y'^2}{w_f^2}\right)\right] \quad \text{..........................(15)}$$

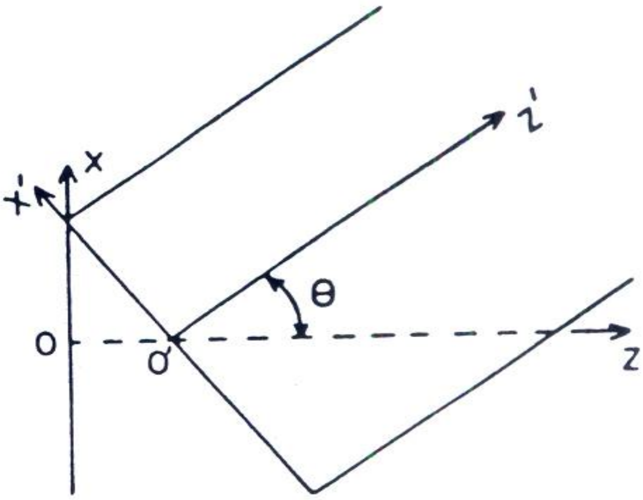

Figure 3: Angular mismatch between the upside down tapered microlens transformed input face and the end face of the fiber.

The coupling efficiency η_a for a small angular mismatch θ in case of circular core fiber is given by [9,11,22]

$$\eta_a = \eta_0 \exp\left[-\frac{k_2^2\theta^2}{2}\left\{\frac{\left(w_f^2+w_{2x}^2\right)w_{2x}^2 w_f^2}{\left(w_f^2+w_{2x}^2\right)^2+\frac{k_2^2 w_{2x}^4 w_f^4}{4R_{2x}^2}}\right\}\right] \quad \text{......................... (16)}$$

where Eqs. (10), (14) and (15) are employed to evaluate coupling losses for angular misalignments.

The above formulations are used in the next section to calculate coupling efficiencies in absence and presence of possible transverse and angular misalignments in case of coupling in between LD and CCGISMF for a specific *V* value corresponding to each profile exponent *g* in refractive index profile.

3. Results and Discussions

3.1. Optogeometrical parameters under consideration

In order to estimate coupling efficiencies in absence and presence of any possible transverse and angular misalignments for a UDTM on the tip of CCGISMF, we use first a LD emitting light of wavelength $\lambda = 1.3\mu m$ with $w_{1x} = 1.081\mu m, w_{1y} = 1.161\mu m$ [4] and then use a LD emitting light of wavelength $\lambda = 1.5\mu m$ with $w_{1x} = 0.843\mu m, w_{1y} = 0.857\mu m$ [4]. The LD parameters used in this investigation are mentioned in Table 1. For the LD emitting light of abovementioned wavelengths, we compute relevant source position with resulting maximum coupling efficiencies for a series of CCGISMFs having different profile exponents *g* (= 1, 2, 4, 8, 10, 20, ∞) [29] in refractive index profile. We choose *V* value corresponding to each *g* value (*g* = 1, 2, 4, 8, 10, 20, ∞) as 1.924 [4]. Different fiber spot sizes w_f for this specific *V* value corresponding to each *g* value (*g* = 1, 2, 4, 8, 10, 20, ∞) [29] are then calculated [25].

Table 1

Laser diode parameters

LD	Wavelength λ in *µm*	Spot size w_{1x} in *µm*	Spot size w_{1y} in *µm*	λ_1 in *µm*	k_2 in μm^{-1}
#1	1.3	1.081	1.161	0.4138	7.4915
#2	1.5	0.843	0.857	0.4775	6.4926

Again as taken in all previous cases, the maximum depth of the microlens *h* is taken as $6\mu m$ [7]. The refractive index $\mu(=\frac{\mu_2}{\mu_1})$ of the material of the microlens with respect to surrounding medium is once again taken as 1.55 [4,7]. The core and cladding refractive indices are chosen as 1.46 and 1.45 respectively. The core diameter is taken as 2*a* = 4 *µm*. An UDTM to be drawn from those typical fibers is chosen with 2*d* = 6 *µm* with UDTM length z_L as 23.3 *µm* corresponding to *L* being 70 *µm*. The radius of curvature R_0 of the spherical end of the UDTM is taken as 90 *µm* [20]. Further, as explained in earlier cases, since estimation of coupling efficiency on the basis of planar wave model differs slightly from that on the basis of spherical wave model [7,8], we consider planar wave model for the input beam from the laser facet for the sake of simplicity.

3.2. Results for coupling scheme without misalignment consideration

It is observed that for LD #2 emitting light of wavelength $\lambda = 1.5\mu m$, the maximum coupling efficiency of 98.19% is excellently achieved for CCGISMF having triangular index profile (*g* =1) for source position 5.5 *µm*. However, for the LD #1 emitting light of wavelength $\lambda = 1.3\mu m$, this promising aspect of maximum coupling efficiency of 99.20% is also similarly supported for fiber with parabolic index profile having profile exponent *g* = 2 for source position of 5.3 *µm*. Hence, the comparison between these results for CCGISMF excited with two wavelengths predicts that fibers with profile exponent *g* = 2 appear to be more suitable in the context of the aforesaid coupling optics involving GIFs and this excitement is uniquely excellent for a LD #1 emitting specially light of wavelength $\lambda = 1.3\mu m$ in absence of any misalignment. But it may be worthwhile to mention that the triangular profile g = 1 possesses dispersion-shifted merit in the lowest loss in wavelength region of λ = 1.5 μm and for more or less same focal length and maximum coupling efficiency stands as a better candidate for technological importance.

3.3. Results with misalignment considerations

Accordingly, in our final part, we use corresponding values of source positions for most efficient CCGISMF with g = 1 and V = 1.924 with w_f of 9.901 μm to estimate coupling efficiencies with transverse and angular misalignments for LD #2 and also for CCGISMF with g = 2 and V = 1.924 with w_f of 6.156 μm excited with LD #1. The respective results for transverse and angular misalignments are reported in Table 2. These investigations of coupling efficiencies are restricted around 0 to 2 μm region for transverse offset and 0 to 2^0 region for angular misalignment [9,11]. This region is chosen in consideration with the fact that designers of microlenses can restrict the fabrication to such small misalignments.

Table 2

Coupling efficiencies with transverse and angular misalignments for graded index fiber excited with LD #1 & LD #2

d = 6.0 μm, μ = 1.55, a = 2.0 μm, D = 3.0 μm, R_0 = 90 μm, L= 70 μm, V = 1.924

λ = 1.3 μm, g = 2					λ =1.5 μm, g = 1				
u (μm)	η_0	η_{10}^*	η_{01}^*	η_a^*	u (μm)	η_0	η_{10}^*	η_{01}^*	η_a^*
5.3	0.9920	0.8882	0.8818	0.5473	5.5	0.9819	0.9378	0.9372	0.3302

From Table 2, it is evident that coupling efficiencies corresponding to transverse and angular misalignments show mutually complemental results. It must be noted in Table 2 that the symbol η_{10}^* indicates coupling coefficient for transverse misalignment of 2 μm along X direction only while η_{01}^* indicates coupling coefficient for transverse misalignment of 2 μm along Y direction only. On the other hand, η_a^* represents coupling coefficient for angular misalignment of 2^0. Now, the calculated no offset value of coupling loss for the fiber with V = 1.924 and g = 2 excited with LD#1 emitting light of wavelength $\lambda = 1.3\mu m$ is obtained as 0.0349 dB. Further, it is evident from Table 2 that the calculated coupling losses for this fiber is 0.5149 dB for transverse misalignments of 2 μm along X direction only. The calculated coupling loss for this specific fiber is 0.5463 dB for transverse misalignments of 2 μm along Y direction only. It is also found that the coupling losses for the said fiber is 2.6178 dB for angular mismatch of 2^0. However, the calculated no offset value of coupling loss for the fiber with V = 1.924 and g = 1 excited with LD #2 emitting light of wavelength $\lambda = 1.5\mu m$ is obtained as 0.0793 dB. Further, it is evident from Table 2 that the calculated coupling losses for this fiber is 0.2789 dB for transverse misalignments of 2 μm along X direction only. The calculated coupling loss for this specific fiber is 0.2817 dB for transverse misalignments of 2 μm along Y direction only. It is also found that the coupling losses for the said fiber is 4.8122 dB for angular mismatch of 2^0. However, as the transverse misalignment is more sensitive than that of angular misalignments, the results for fiber with g = 1 and V = 1.924 are most suitable when excited with LD emitting light of wavelength $\lambda = 1.5\mu m$ as far as misalignments are considered.

It is relevant to mention in this connection that V =1.924 value really corresponds to low V region for triangular index fiber which has the first higher order mode cut off frequency of V_{c1} = 4.38 as well as for parabolic index fiber for which first higher order mode cut off frequency of V_{c1} = 3.5. This low V region is very well known for evanescent wave coupling. Therefore if one likes to exploit our results for use in optical directional couplers they can easily choose such region of V for practical purpose.

Then, for fiber with V = 1.924 corresponding to profile exponent g = 2 excited with LD #1 emitting light of wavelength $\lambda = 1.3\mu m$ and corresponding to profile exponent g = 1 excited with LD #2 emitting light of wavelength $\lambda = 1.5\mu m$, we present the variation of coupling efficiencies versus the transverse misalignments in Figures 4 and 5 respectively for the typical estimation of knowledge of excitation via UDTM in presence of transverse misalignments. The coupling efficiency designated as EFF10 is represented by the dashed line (corresponding to d_2 = 0 with d_1 varying from 0 to 2 μm) while the coupling efficiency EFF01 is represented by the solid line (corresponding to d_1 = 0 with d_2 varying from 0 to 2 μm). In Figures 6 and 7, the curves present the variation of coupling efficiencies with the angular mismatch for the said most efficient fibers excited with same LDs emitting light of wavelength $\lambda = 1.3\mu m$ and $\lambda = 1.5\mu m$, respectively.

Although step index fiber is usually used for communication, GIF having dispersion-shifted criteria stands as a potential candidate for its zero dispersion wavelength being shifted to the region of 1.55 μm to exploit the well known low loss window. Further, triangular index profile has a strong dispersion-shifted merit. Side by side, it may be relevant to mention in this connection that the wavelength at and around 1.5 μm is the region where the erbium doped fiber amplifier and Raman gain fiber amplifier efficiently and elegantly operate. Coupled with these favourable factors for the 1.5 μm wavelength region, one can recommend use of CCGISMF having triangular index profile (g = 1) safely as a microlensing scheme in optimum coupling optics. It is important to note that the source position is nearly constant in both cases. Our present analysis and results point out the merit of triangular index profile in coupling of LD and CCGISMF via UDTM and present the relevant optimum coupling optics. However, the assembly of a LD in the close proximity of the UDTM within 5.3 μm is challenging to achieve in practice. But with the advent of new progress in nanotechnology, we are optimistic that the future technologist will involve any breakthrough to realize our result and test it experimentally.

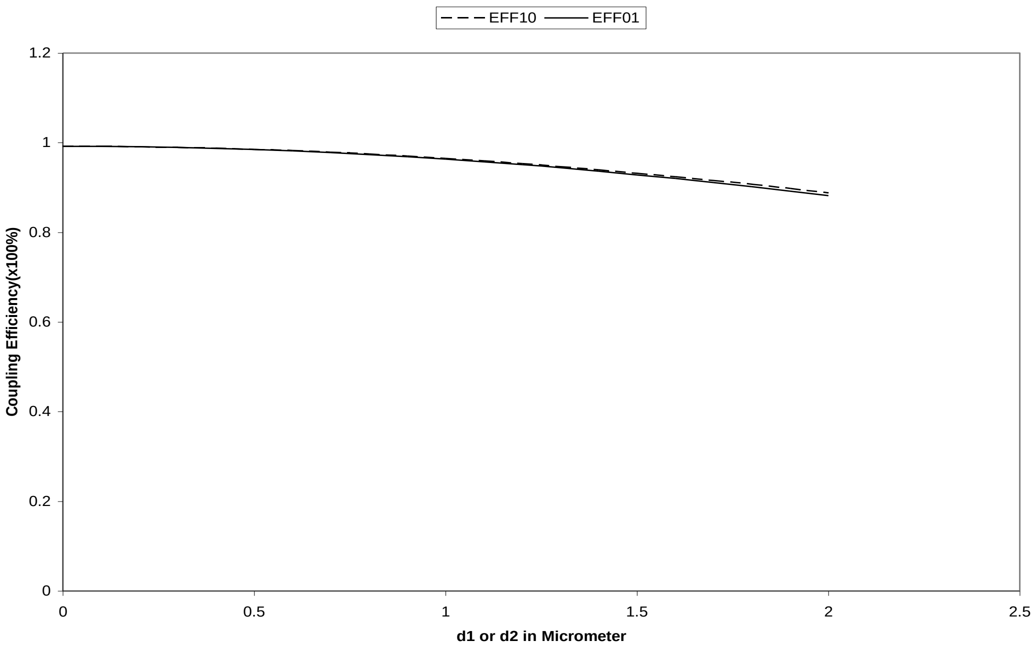

Figure 4: Variation of coupling efficiencies with the transverse misalignment for fiber having g = 2, V = 1.924 and w_f of value 6.156 μm excited with LD #1. The coupling efficiency designated as EFF10 is represented by the dashed line (corresponding to d_2 = 0 with d_1 varying from 0-2 μm) while the coupling efficiency EFF01 is represented by the solid line (corresponding to d_1 = 0 with d_2 varying from 0-2 μm).

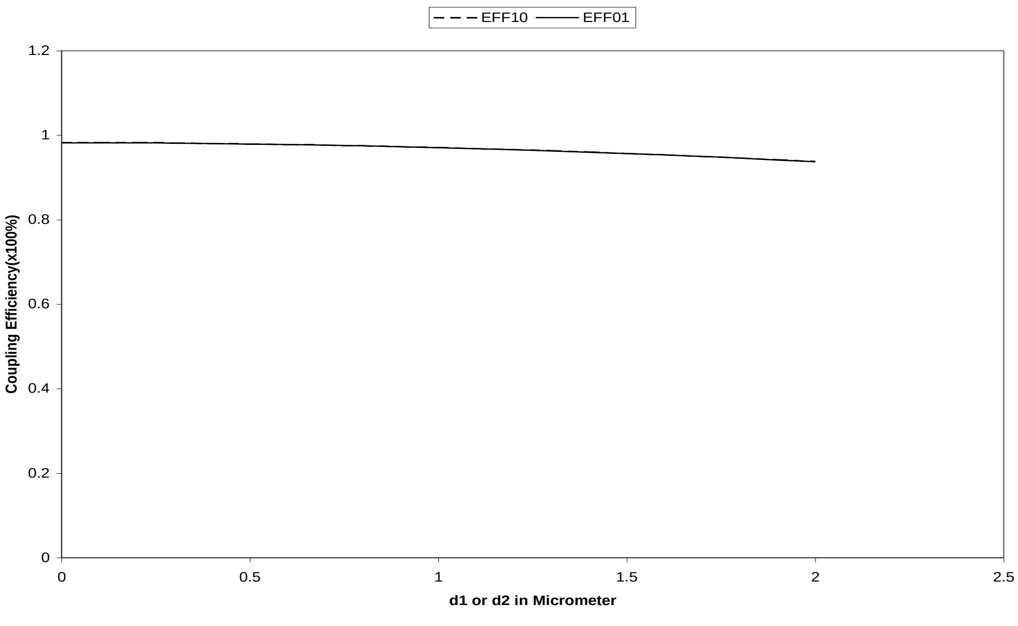

Figure 5: Variation of coupling efficiencies with the transverse misalignment for fiber having g = 1, V = 1.924 and w_f of value 9.901 μm excited with LD #2. The coupling efficiency designated as EFF10 is represented by the dashed line (corresponding to d_2 = 0 with d_1 varying from 0-2 μm) while the coupling efficiency EFF01 is represented by the solid line (corresponding to d_1 = 0 with d_2 varying from 0-2 μm).

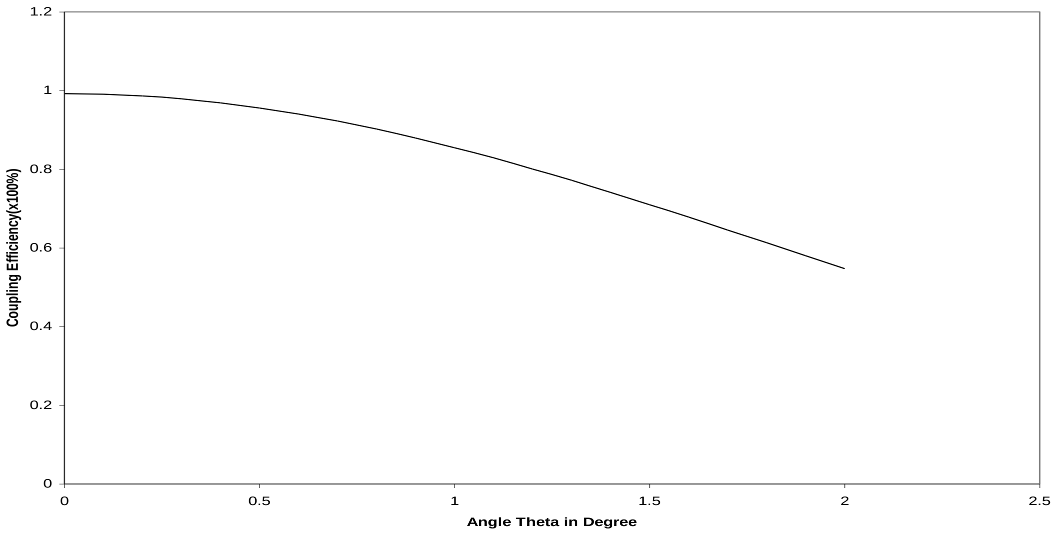

Figure 6: Variation of coupling efficiency with the angular misalignment for fiber having *g* = 2, *V* = 1.924 and w_f of value 6.156 μm excited with LD #1.

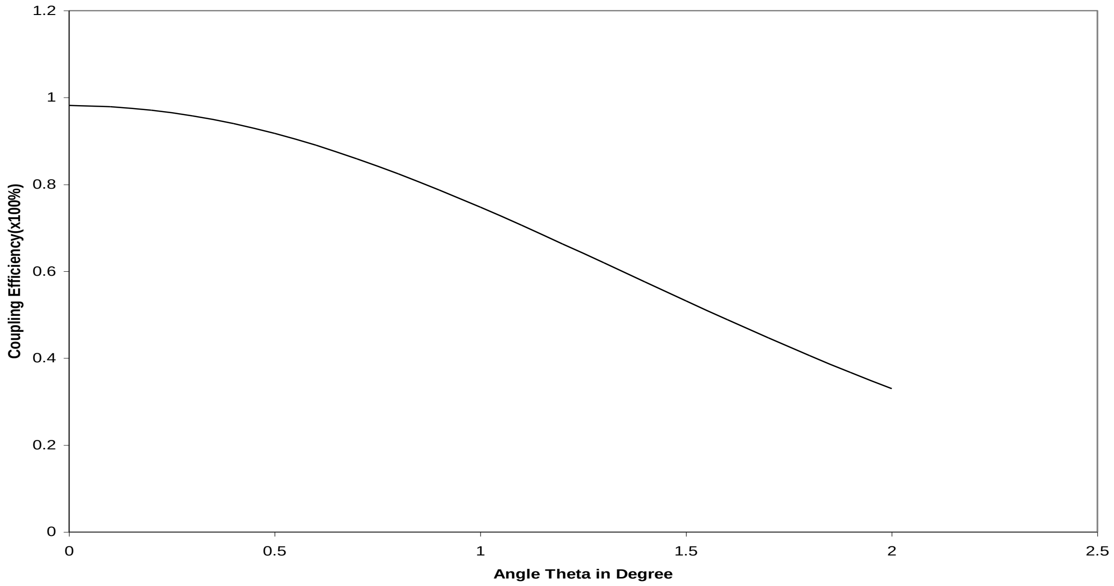

Figure 7: Variation of coupling efficiency with the angular misalignment for fiber having *g* = 1, *V* = 1.924 and w_f of value 9.901 μm excited with LD #2.

4. Conclusion

The coupling optics in case of source to CCGISMF excitation via UDTM on the fiber tip has been studied in presence of possible transverse and angular mismatches. The study has been performed using laser sources emitting two practically interesting different wavelengths of 1.3 μm *and* 1.5 μm respectively. For fibers with a typical *V* value corresponding to each profile exponent *g* value, appropriate source positions are chosen so as to give maximum coupling for the respective fiber. The best maximum coupling is achieved for triangular index fibers when excited with LD emitting light of wavelength $\lambda = 1.5\mu m$. The application of

ABCD matrix has simplified the analysis and the concerned calculations need little computations. Such study which as per our knowledge is the first theoretical investigation, should be extremely useful for the designers and packagers of the microlenses on the fiber tip. The results are also extremely useful for assessing deeply the sensitivity of such coupler with reference to above kind of misalignments. However, the designers and packagers should be more careful in order to avoid angular mismatches as is visualized that a little angular misalignment causes a pronounced setback in comparison with little transverse misalignment.

Appendix:

Considering the distance *u* of the LD from the UDTM end, *q* parameters of the Gaussian beams at the input laser facet and the output microlens fiber interface can be related by the ABCD matrix as follows:

The input and output parameters (q_1,q_2) of the light beam is related by [20]

$$q_2 = \frac{Aq_1 + Au + B}{Cq_1 + Cu + D} \quad \text{(A1)}$$

where

$$\frac{1}{q_{1,2}} = \frac{1}{R_{1,2}} - \frac{i\lambda_0}{\pi w_{1,2}^2 \mu_{1,2}} \quad \text{(A2)}$$

The ray matrix *M* for the UDTL on the fiber tip is given by [19,20]

$$M = \begin{pmatrix} A & B \\ C & D \end{pmatrix} \quad \text{(A3)}$$

where

$$A = r_2(z) - \frac{(1-\mu) r_1(z)}{\mu R_0} \quad \text{(A4a)}$$

$$B = \frac{r_1(z)}{\mu} \quad \text{(A4b)}$$

$$C = -\frac{(1-\mu)}{\mu R_0}\frac{dr_1(z)}{dz} + \frac{dr_2(z)}{dz} \quad \text{(A4c)}$$

$$D = \frac{1}{\mu}\frac{dr_1(z)}{dz} \quad \text{(A4d)}$$

The refractive index of the material of the microlens with respect to the incident medium is represented by $\mu (= \mu_2 / \mu_1)$.

The *z* dependence of the above matrix elements can be explicitly expressed by substituting [19,20]

$$r_1(z) = -\frac{L}{\alpha}\left(1-\frac{z}{L}\right)^{1/2}\sin k(z) \qquad \text{(A5a)}$$

$$\frac{dr_1(z)}{dz} = \frac{1}{\left(1-\frac{z}{L}\right)^{1/2}}\left\{\cos k(z) + \frac{1}{2\alpha}\sin k(z)\right\} \qquad \text{(A5b)}$$

$$r_2(z) = \left(1-\frac{z}{L}\right)^{1/2}\left\{\cos k(z) - \frac{1}{2\alpha}\sin k(z)\right\} \qquad \text{(A5c)}$$

$$\frac{dr_2(z)}{dz} = \frac{A_0^2 L}{\left(1-\frac{z}{L}\right)^{1/2}\alpha}\sin k(z) \qquad \text{(A5d)}$$

where, $k(z) = \alpha \ln\left(1-\frac{z}{L}\right)$ ……………………………………………….. (A6a)

and $\alpha = \left(A_0^2 L^2 - 1/4\right)^{1/2}$ ……………………………………(A6b)

L being the tapered length or length of the cone including tapered region and A_0 is a constant given by

$$A_0 = \frac{1}{d}\left(2\ln\frac{n_{core}}{n_{clad}}\right)^{1/2} \qquad \text{(A7)}$$

For a UDTM having aperture 2*d*

$$z_L = \frac{L(d - a)}{d} \qquad \text{(A8)}$$

In order to obtain $w_{2x,2y}$, the matrix is evaluated for $z = z_L$.

The transformed beam spot sizes and radii of curvature in the X and Y directions are found by using Eqs. (A4a-A4d) in Eqs. (A1) and (A2) and are given by

$$w_{2x,2y}^2 = \frac{A_1^2 w_{1x,1y}^2 + \frac{\left(\lambda_1^2 B_1^2\right)}{\pi^2 w_{1x,1y}^2}}{\mu(A_1 D_1 - B_1 C_1)} \qquad \text{(A9)}$$

$$\frac{1}{R_{2x,2y}} = \frac{A_1 C_1 w_{1x,1y}^2 + \frac{\left(\lambda_1^2 B_1 D_1\right)}{\pi^2 w_{1x,1y}^2}}{A_1^2 w_{1x,1y}^2 + \frac{\left(\lambda_1^2 B_1^2\right)}{\pi^2 w_{1x,1y}^2}} \qquad \text{(A10)}$$

where $\lambda_1 = \frac{\lambda_0}{\mu_1}$ ……………………………………………(A11)

$$A_1 = A + \frac{B_1}{R_1} \qquad \text{(A12a)}$$

$B_1 = Au + B$ **……………………………………………** (A12b)

$C_1 = C + \frac{D_1}{R_1}$ **……………………………………….. (A12c)**

$D_1 = Cu + D$ **………………………………………..**(A12d)

In plane wavefront model, the radius of curvature R_1 of the wavefront from the laser facet →∞. This leads to $A_1=A$ and $C_1=C$.

Acknowledgement: The author is grateful to University Grants Commission(UGC) for providing financial assistance in a UGC-Minor Research Project (Sanc. No. PSW-076/14-15 (ERO)). He is also grateful to Prof. S.N. Sarkar, Professor of the Department of Electronic Science, University of Calcutta for his helpful discussions and constant encouragement.

References:

1. J. H. Song *et al.*, *J. Lightwave Technol***.**, **27,** 1533-1539 (2009).
2. H.M. Presby and C.A. Edwards, *Electron. Lett.,* **28,** 582-584 (1992).
3. C.A. Edwards *et al.*, *J. Lightwave Technol.*, **11,** 252-257 (1993).
4. J. John *et al.*, *IEE Proc. Optoelectron.*, **141,** 178-184 (1994).
5. H. Liu *et al.*, *Appl. Opt.*, **44**, 4809-4813 (2005).
6. H. Liu, *Optik*, **119**, 666-670 (2008).
7. S. Gangopadhyay and S.N. Sarkar, *Opt. Commun.*, **132,** 55-60 (1996).
8. S. Gangopadhyay and S.N. Sarkar, *Appl. Opt.*, **36,** 8582-8586 (1997).
9. S. Gangopadhyay and S.N. Sarkar, *Opt. Commun.*, **146,** 104-108 (1998).
10. S. Gangopadhyay and S.N. Sarkar, *J. Opt. Commun.*, **19**, 42-44 (1998).
11. S. Gangopadhyay and S.N. Sarkar, *J. Opt. Commun.*, **19**, 217-221 (1998).
12. S. Mukhopadhyay *et al.*, *Opt. Eng.*, **46(2),** 025008(1-5) (2007).
13. S. Mukhopadhyay *et al.*, *Opt. Eng.*, **46(9),** 095008(1-5) (2007).
14. M.C. Kundu and S. Gangopadhyay, *Optik,* **117**, 586-590 (2006).
15. P. Patra *et al.*, *Optik*, **119,** 596-600 (2008).
16. A. W. Snyder and J. D. Love, " *Optical Waveguide Theory*" , Chapman and Hall Limited, London (1983).

17. L.B. Yuan and R.L. Shou, *Sensors and Actuators*, **A21-A23**, 1158-1161 (1990).
18. L.Yuan and A. Qui, *J. Opt. Soc. Am. A*, **9**, 950-952 (1992).
19. S. K. Mondal *et al.*, *Appl. Opt.*, **37**, 1006-1009 (1998)**.**
20. S. K. Mondal and S.N. Sarkar, *Appl. Opt*,. **38**, 6272-6277 (1999).
21. S. Mukhopadhyay *et al.*, *Optik*, **121,** 142-150 (2010).
22. S. Mukhopadhyay and S.N. Sarkar, *Opt. Eng.*, **50(4),** 045004 (1-9) (2011).
23. A. Bose *et al.*, *J. Opt. Commun.*, **33(1),** 15-19 (2012).
24. A.K. Ghatak and K. Thyagarajan, Chapter 13, pp 411-415 in " *Optical Electronics*", Cambridge University Press, United Kingdom (1998).
25. D. Marcuse, *J. Opt. Soc. Am.*, **68**, 103-109 (1978).
26. D. Marcuse, *J. Bell Syst. Tech.*, **56**, 703-718 (1977).
27. S.N. Sarkar *et al.*, *J. Opt. Commun.*, **7**, 92-96 (1986).
28. S. Sarkar *et al.*, *Opt. Commun.*, **49**, 178-183 (1984).
29. R. Tewari and B.P. Pal, *J. Opt. Commun.*, **6**, 25-29 (1985).